

Effect of Ball-Milling on Porous Structure of Ca-Substituted Leucite Porous Body with Low Thermal Expansion Coefficient

Ikuo YANASE, Yoichi ISHIKAWA and Hidehiko KOBAYASHI

Department of Applied Chemistry, Faculty of Engineering, Saitama University,
255, Shimo-ohkubo, Sakura-ku, Saitama-shi, Saitama 338-8570

低熱膨張 Ca 置換 リューサイト多孔体の細孔構造に及ぼすボールミル効果

柳瀬郁夫・石川洋一・小林秀彦

埼玉大学工学部応用化学科, 338-8570 埼玉県さいたま市桜区下大久保 255

The ball-milling for amorphous calcined powder in a PMMA solution, prepared by heating a mixture of nitrates, γ -Al₂O₃, and amorphous SiO₂ powders were effective for the fabrication of Ca-substituted leucite porous bodies with almost homogeneous pore-size distributions. Especially, when the amorphous powder calcined at 1073 K was ball-milled for 48 h, the pore size decreased to 0.159 μ m and porosity increased in the porous body fabricated using the amorphous calcined powder. The FT-IR spectroscopy revealed that the amorphous calcined powder is composed of fine particles having a network of (Si, Al)O₄ tetrahedra similar to the aluminosilicate framework of the leucite compounds. The fabricated porous body showed a low linear thermal expansion coefficient of $1.405 \times 10^{-6}/\text{K}$ in the temperature range of 298 to 1273 K.

[Received May 12, 2006; Accepted September 21, 2006]

Key-words : Ballmill, Amorphous phase, FT-IR, Porous structure, Calcium, Thermal expansion

1. Introduction

Porous ceramics are very useful in capturing particulate matter (PM) that can have adverse effects on human health.^{1)–3)} This PM is found in exhaust gases derived from automobiles, factories and other sources. PM is classified into two groups on the basis of their diameter; particles with a diameter $\leq 2.5 \mu\text{m}$ are called PM 2.5, and those with a diameter $\leq 1.0 \mu\text{m}$ are called PM 1. The difference between particles of each size demands the development of ceramic filters with pores of controlled size. Additionally, it is important that ceramic filters have low thermal expansion coefficient and a high thermal stability, because the PM captured in ceramic filters must be combusted at higher temperatures and then cooled for the ceramic filters to be reused.

An aluminosilicate porous body of cubic Cs-deficient pollucite,⁴⁾ Cs_{0.9}Al_{0.9}Si_{2.1}O₆, with a linear thermal expansion coefficient of ca. $1.0 \times 10^{-6}/\text{K}$ in the range of 298 to 1273 K, would be an attractive candidate as a novel ceramic filter for capturing PM, because aluminosilicate does not have serious problems of oxidation at higher temperatures. It also does not produce microcracks due to thermal stress from anisotropic thermal expansion as does cordierite, Mg₂Al₄Si₅O₁₈, which is problematic because microcracks are produced during its regeneration.⁵⁾

The fabricated porous body of Cs_{0.9}Al_{0.9}Si_{2.1}O₆ has several sizes of pores producing a wider range of diameters from ca. 0.2 to 5.5 μm , which means that pore-size control is not achieved to the extent required.⁴⁾ Such heterogeneous pore formation is considered to be due to the agglomerated particles in the calcined powder, suggesting that grinding the agglomerates is effective for the formation of a homogeneous porous structure. However, a highly controlled porous structure could not be obtained by ball-milling the Cs_{0.9}Al_{0.9}Si_{2.1}O₆ powder calcined at 1073 K whereas the porosity of the porous body increases.⁴⁾

In this work, a cation with a different valence was substitut-

ed for the cesium ion in Cs_{0.9}Al_{0.9}Si_{2.1}O₆. This substitution was expected to suppress the crystallization of a leucite phase, resulting in produce of the calcined powder with an amorphous phase, which is easily ground by ball-milling. The thermal shrinkage of a compact of the amorphous calcined powder and the porous structure of the porous bodies fabricated were investigated by a thermal mechanical analysis (TMA), a scanning electron microscopy (SEM), and Hg intrusion porosimetry. Furthermore, the thermal expansion coefficient of the porous bodies fabricated was measured by TMA.

2. Experimental

2.1 Preparation of Ca-substituted pollucite powder

Ca(NO₃)₂·4H₂O powder (>99%; High Purity Co., Ltd.), CsNO₃ powder (>99%; High Purity Co., Ltd.), Al₂O₃ sol (alumina sol 200; Nissan Chemical Co., Ltd.) and SiO₂ sol (snotex O; Nissan Chemical Co., Ltd.) were used as raw starting materials. First, Al₂O₃ and SiO₂ sols were mixed at pH = 5.4, dried, and heated at 873 K in air for 20 h to obtain a mixed fine powder of γ -Al₂O₃ and amorphous SiO₂ (molar ratio of Al/Si = 0.9/2.1).⁶⁾ Second, CsNO₃ and Ca(NO₃)₂·4H₂O powders were added to the fine powder mixture of γ -Al₂O₃ and amorphous SiO₂ to give a molar ratio of 0.74/2.1 for Cs/Si and of 0.08/2.1 for Ca/Si in the case of the Ca-substituted powder with a chemical formula of Cs_{0.74}Ca_{0.08}Al_{0.9}Si_{2.1}O₆ and to give a molar ratio of 0.9/2.1 for Cs/Si in the case of the non-substituted powder with a chemical formula of Cs_{0.9}Al_{0.9}Si_{2.1}O₆. The mixed powders were heated at 873 K in air for 20 h to decompose CsNO₃ and Ca(NO₃)₂. Then the powders consisting of an amorphous phase were calcined at 1073 and 1273 K in air for 20 h to investigate the crystallization process. Here, the ideal densities calculated from lattice constants of the crystalline Cs_{0.74}Ca_{0.08}Al_{0.9}Si_{2.1}O₆ (hereafter, CCAS) and Cs_{0.9}Al_{0.9}Si_{2.1}O₆ (hereafter, 9CAS) were 2.93 and 3.10 g/cm³, respectively.

2.2 Fabrication of Ca-substituted pollucite porous bodies

The powders calcined at 1073 K were well-dispersed in acetone by an ultrasonic treatment. Then polymethyl methacrylate (PMMA; $(C_5H_8O_2)_n$, Wako Co., Ltd.) were dissolved in acetone and mixed with the calcined powder for 24, 36, and 48 h by ball-milling. The size of the Al_2O_3 balls used for the ball-milling was 5 mm ϕ in diameter. The ratio of PMMA added to the calcined powders was 35 mass% of the value that had been optimized previously.⁴⁾ Green compacts composed of the calcined powders and 35 mass% PMMA were prepared by anisotropic pressing at 49 MPa for 1 min, followed by cold isostatic pressing (CIP) at 196 MPa also for 1 min. The specimen was approximately 5 \times 5 \times 10 mm³. The compact prepared was heated at 873 K in air for 20 h to decompose and delete the PMMA at a heating rate of 2 K/min, according to the condition that the PMMA in a green compact composed of amorphous leucite powder could be decomposed and deleted in the temperature range of 523 to 773 K, which was clarified by a TG-DTA measurement in our previous paper.⁷⁾ Then the preheated specimens were sintered at 1473 K in air for 20 h to fabricate the porous bodies of CCAS.

2.3 Evaluations

The calcined powders were examined by a X-ray diffraction (XRD; Rad-C, Rigaku Co., Ltd., Cu K α , 40 kV, 30 mA) analysis and by a Fourier transform infrared spectroscopy (FT-IR; IRPrestige-21, Shimadzu Co., Ltd.) with the KBr method. Thermal expansion properties of the synthesized CCAS and 9CAS powders were investigated in the viewpoint of the lattice parameter by a high temperature X-ray diffractometer equipment (HTXRD; Mac Science, MXP18VA, Cu K α , 40 kV, 200 mA). Lattice parameters of the synthesized CCAS and 9CAS were refined at temperatures ranging between 298 to 1173 K, by the least-squares method, using six diffraction peaks of (332), (440), (532), (631), (721) and (732) planes. These diffraction peak positions were corrected using a commercial Si powder (99.9% up, High Purity Chemical Lab. Co., Ltd.) as the external standard, at a scanning speed of 1 $^\circ$ /min in the scanning 2θ range of 20 to 80 $^\circ$. A measuring sample was set in a Pt holder in contact with the thermocouple in the HTXRD apparatus. The thermal shrinkage behavior in the temperature range of 298 to 1473 K of the compacts of Ca-substituted and non-substituted pollucites heated at 873 K for 20 h to decompose PMMA was investigated by a thermomechanical analyzer (TMA 8310, Rigaku Co., Ltd.), using an Al_2O_3 rod as a reference. The fractured surfaces of the porous bodies were observed using SEM (S4100, Hitachi, Co., Ltd.). The porosity of the open pores and the pore-size distributions of the porous bodies were investigated using a Hg intrusion porosimetry (Autopore 9520, Shimadzu Co., Ltd.). The thermal expansion behavior in the temperature range of 298 to 1273 K of the fabricated porous body was measured by TMA, using SiO_2 glass rod as a reference.

3. Results and discussion

3.1 Characterization of Ca-substituted calcined powders

XRD patterns of non-substituted (hereafter 9CAS) and the Ca-substituted (hereafter CCAS) leucite powders calcined at 873, 1073, and 1273 K for 20 h are shown in Figs. 1(a) and (b), respectively. Here, these calcined powders were not ball-milled for grinding. The 9CAS and CCAS powders calcined at 873 K (hereafter 873 K-calcined powder) had an amorphous phase without any diffraction peaks, suggesting that the calcined powders are highly reactive during sintering. Actually, we succeeded in fabricating the dense sintered bodies of 9CAS using an amorphous calcined powder.⁸⁾ However, there was

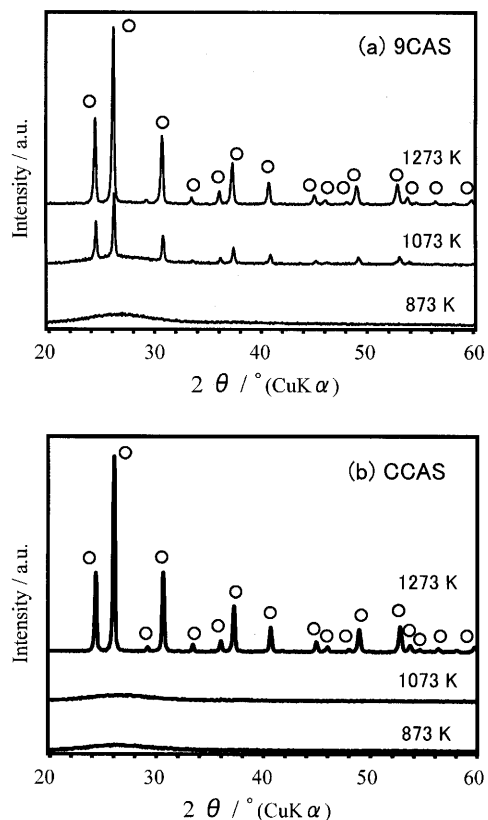


Fig. 1. XRD patterns for powders of 9CAS (a) and CCAS (b) calcined at temperatures : 873 K, 1073 K, and 1273 K.

the difference between 9CAS and CCAS at 1073 K that CCAS displayed an amorphous phase and 9CAS, a crystalline phase in the XRD patterns, which means that the crystallization of the Cs-leucite compound, $Cs_{0.9}Al_{0.9}Si_{2.1}O_6$, in the calcined powder was suppressed by the Ca substitution. Finally, it was confirmed that both the calcined powders had the single phase of Cs-leucite related compounds from XRD patterns. Figures 2(a) and (b) show thermal expansion properties in the temperature range of 298 to 1273 K of 9CAS and CCAS powders with a crystalline single phase, respectively. CCAS showed a linear thermal expansion property compared to 9CAS and its thermal expansion rate was almost equal to that of 9CAS. Thus it was found that Ca-substitution for 9CAS was achieved without losing an advantage of the lower thermal expansion property of 9CAS.

The FT-IR spectra of the powder calcined at temperatures: (b) 1073 K, (c) 1273 K, and (d) 1473 K, are shown in Fig. 3, together with the spectrum (a) of a mixed fine powder composed of amorphous SiO_2 and $\gamma-Al_2O_3$ at a molar ratio of Si/Al=2.1/0.9, with XRD pattern of an amorphous phase. As for the spectrum (b) of the powder calcined at 1073 K (hereafter 1073 K-calcined powder), no absorption peak due to NO_3^- was observed in the spectrum, showing that the 1073 K-calcined powder contained no undecomposed nitrates from the starting materials. However, a significant difference in the peak shape between spectra (a) and (b) was recognized. As for the spectrum (a) of the mixed fine powder of amorphous SiO_2 and $\gamma-Al_2O_3$, absorption peaks in the range of 1300–1000 cm^{-1} are assigned to the asymmetric stretching vibration of Si–O, a peak at ca. 800 cm^{-1} is assigned to the symmetric stretching vibration of Si–O, and a peak at ca. 470 cm^{-1} is assigned to the asymmetric bending vibration of O–Si–O.^{9)–11)}

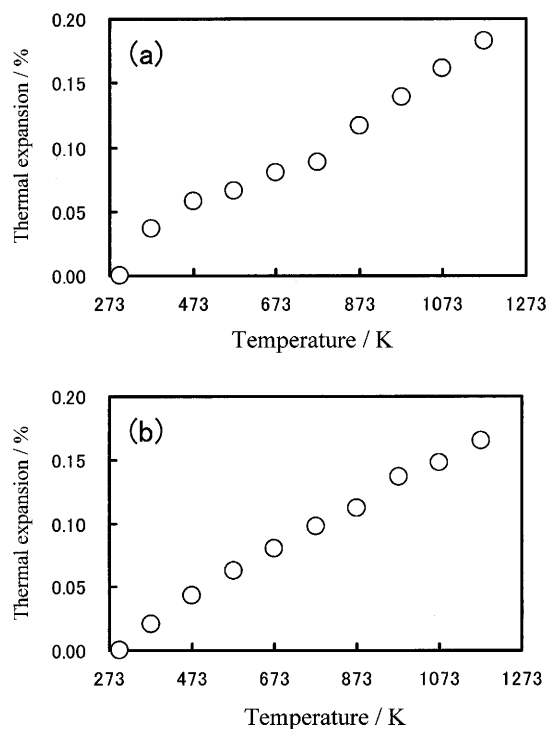


Fig. 2. Thermal expansion properties in the temperature range of 298 to 1173 K for powders of 9CAS (a) and CCAS (b).

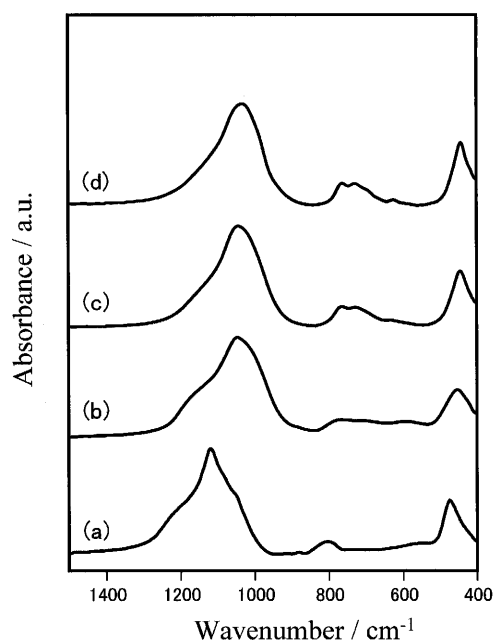


Fig. 3. FT-IR spectra of mixed fine powders of γ - Al_2O_3 and amorphous SiO_2 (a), 1073 K-calcined powder (b), 1273 K-calcined powder (c), 1473 K-calcined powder (d).

No absorption peaks corresponding to γ - Al_2O_3 were clearly observed. In spectrum (b) of the 1073 K-calcined powder, the absorption peak for the asymmetric stretching vibration shifted toward a lower wavenumber. The FT-IR spectrum (c) of the 1273 K-calcined powder with an asymmetric O-(Si,Al)-O stretching vibration¹²⁾ at ca. 1100 cm^{-1} , with a crystallized leucite phase as shown in Fig. 1, suggests that a network of

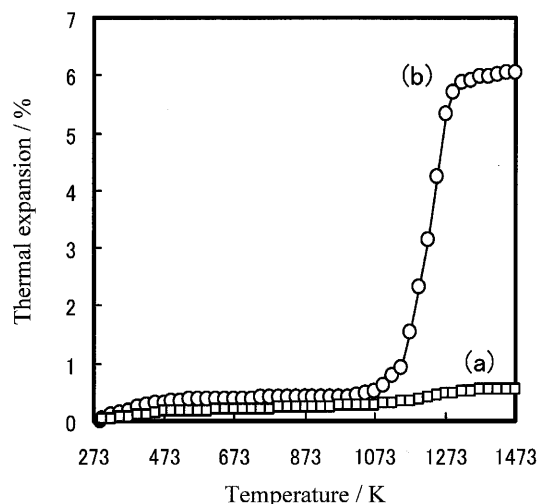


Fig. 4. Thermal shrinkage behaviors in the temperature range of 298 to 1473 K of 9CAS (a) and CCAS (b).

(Si,Al) O_4 tetrahedra was produced in the 1073 K-calcined powder by the reaction of amorphous SiO_2 and γ - Al_2O_3 caused by the thermal decomposition of nitrates. No absorption peak at ca. 800 to 650 cm^{-1} corresponding to the symmetric stretching vibration of O-(Si,Al)-O, which leucite-related compounds have,¹²⁾ was clearly observed in spectrum (b) because the leucite phase was not crystallized.

Figure 4 shows the thermal shrinkage behaviors of compacts of the 1073 K-calcined powders for CCAS and 9CAS in the temperature range of 298 to 1473 K. CCAS specimens began to shrink at ca. 1050 K, and a rapid shrinkage was recognized in the temperature range of 1050 to 1300 K, while 9CAS did not show a marked shrinkage in the same temperature range. This result shows that the calcined powder with an amorphous phase achieved by Ca substitution for Cs-leucite is effective for the fabrication of porous bodies at low temperatures compared with non-substituted Cs-leucite.

3.2 Effect of ball-milling on porous structures

Porous bodies of CCAS were fabricated from the 1073 K-calcined powder with an amorphous phase and ball-milled for 24, 36, and 48 hrs, and then the fractured surfaces of the fabricated porous bodies were investigated to clarify the effect of ball-milling on their microstructure. The SEM photographs shown in Fig. 5 reveal that the microstructure of porous bodies varies with ball-milling time, and increasing the time, decreases the size of the grains together with the size of the pores in the porous bodies. Furthermore, neck formation due to sintering among the grains was observed in the porous bodies fabricated via ball-milling times of 24, 36, and 48 h.

Figure 6 shows the pore size distributions of porous bodies investigated by a Hg-intrusion method. The porous bodies fabricated via ball-milling had different pore-size distributions. In the case of the 24 h-ball-milling, a smaller pore size of $0.71\text{ }\mu\text{m}$ and a larger pore size of $2.57\text{ }\mu\text{m}$ were recognized in the porous bodies. On the other hand, the porous bodies fabricated by 36 h-ball-milling had an almost uniform pore-size distribution with a smaller pore size of $0.375\text{ }\mu\text{m}$, suggesting that the ball-milling ground and decreased the agglomerated particles in the calcined powder. Furthermore, the pore size in the case of the 48 h-ball-milling decreased to $0.159\text{ }\mu\text{m}$ in a smaller pore size and to $0.643\text{ }\mu\text{m}$ in a larger pore size, compared with porous bodies fabricated via the 24 h-ball-milling. Thus, the

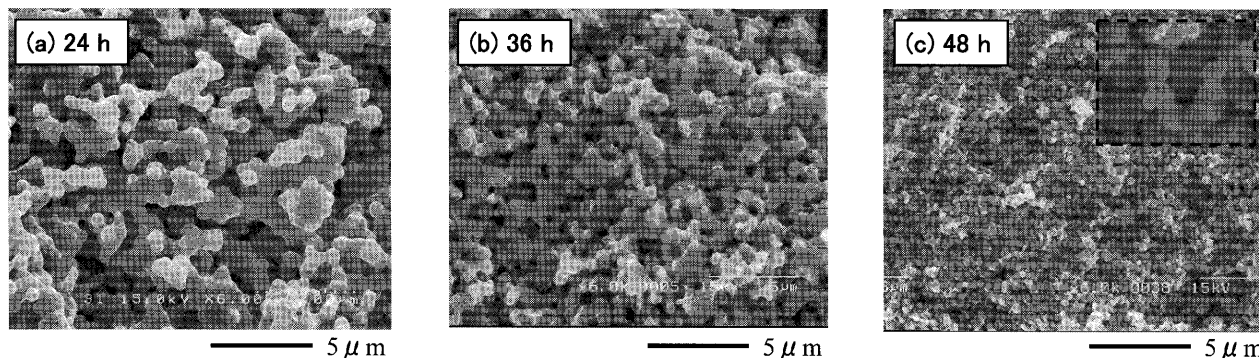


Fig. 5. SEM photographs of fractured surfaces of the porous bodies fabricated via ball-milling for 24 h (a), 36 h (b), and 48 h (c) with a magnified image on the upper right.

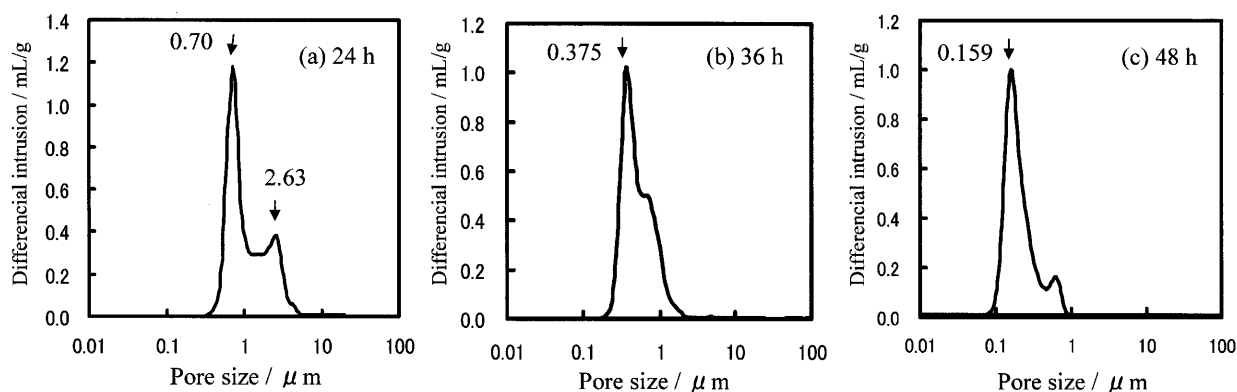


Fig. 6. Pore size distributions of the porous bodies fabricated via ball-milling for 24 h (a), 36 h (b), and 48 h (c).

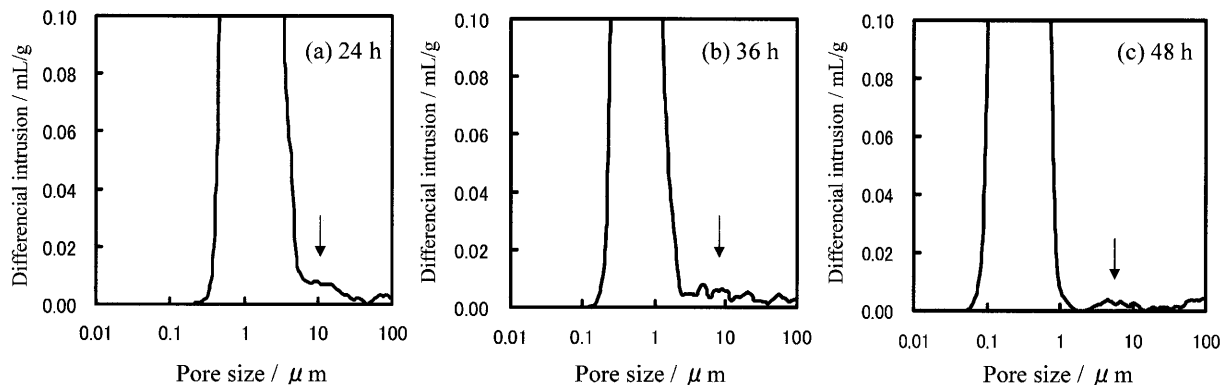


Fig. 7. Larger pore-size distribution of the porous bodies fabricated via ball-milling treatment for 24 h (a), 36 h (b), and 48 h (c).

ball-milling was effective for decreasing pore size because the amorphous calcined powder consisting of agglomerated particles was ground to fine particles and dispersed in acetone during ball-milling. The larger pores remaining in each porous body ball-milled were derived from agglomerated particles insufficiently ground under each condition. To investigate pores larger than the main pores, a magnified scale on the pore-size distribution is shown in Fig. 7. Very small amount of pores were recognized, and the size and the amount of the larger pores decreased with increasing the ball-milling time. The result indicates that the ball-milling treatment for the calcined powder brought about homogeneous pore-size distribu-

tion even in a larger scale.

Figure 8 shows the thermal shrinkage behaviors of the degreased compacts fabricated via ball-milling treatment for 24, 36, or 48 h for the calcined powder. A remarkable thermal shrinkage was observed above 1073 K, which was the calcination temperature of the mixed raw powders. The thermal shrinkages of the specimens varied above 1223 K, and the rate decreased as the ball-milling time increased. The above result suggests that agglomerated particles in the compacts partially enhanced sintering among the agglomerated particles, and led to a large thermal shrinkage as shown in (a) of Fig. 8. On the other hand, thermal shrinkage of the specimen fabricated via

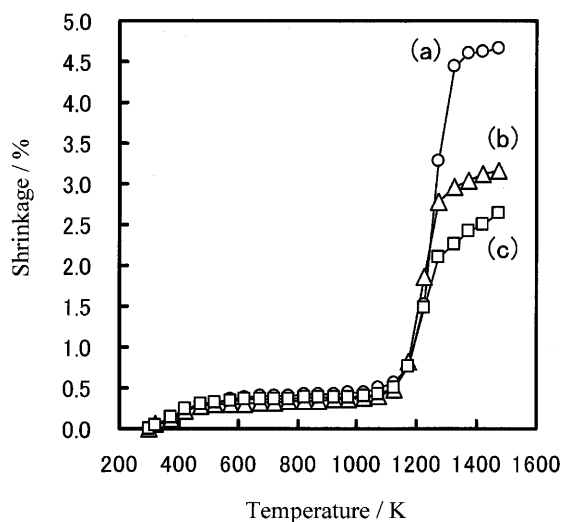


Fig. 8. Thermal shrinkage behaviors in temperature range of 298 to 1473 K of the compacts fabricated via ball-milling treatment for the calcined powder for 24 h (a), 36 h (b), and 48 h (c).

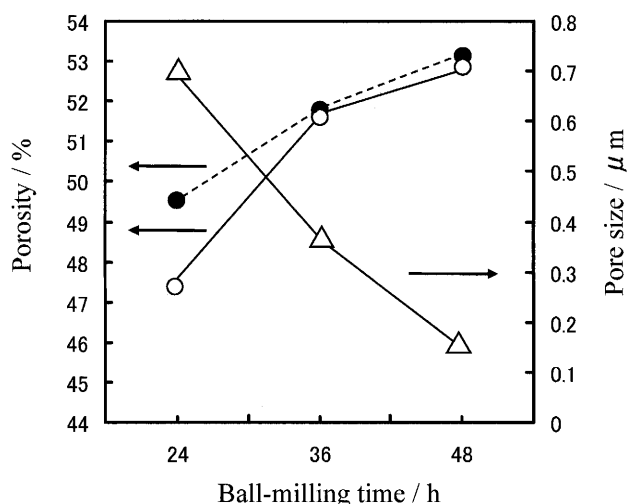


Fig. 9. Effects of time of the ball-milling on porosity and pore size in the porous body. Open and solid circles denote porosities obtained by the Hg intrusion method and by the ideal density of CCAS, respectively, and the triangles denote the main pore size in the porous body obtained by Hg intrusion.

ball-milling for 48 h was suppressed in comparison with the case of ball-milling for 24 and 36 h, suggesting that the amount of the agglomerated particles were decreased efficiently.

Variations in porosity and smaller pore-sizes of fabricated porous bodies versus ball-milling time for calcined powder are shown in Fig. 9. The porosity increased from 47.4 to 52.9% as the ball-milling time increased, regardless of pore-size decreasing. The result indicates that fine particles produced by ball-milling did not enhance grain growth, but they promoted sintering among particles to produce smaller pores, resulting in a higher porosity for the porous body. From the above result, it was considered that PMMA dissolved in acetone deposits heterogeneously among the calcined particles when many agglomerated particles exists in the calcined powder, and that thermal decomposition of the heterogeneous PMMA in the

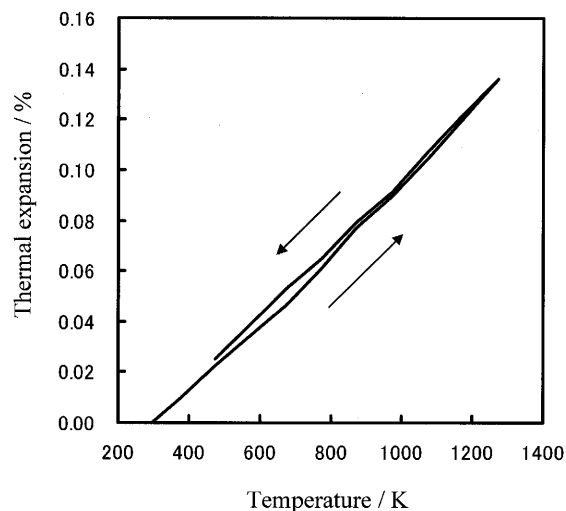


Fig. 10. Thermal expansion property for the fabricated porous body in the temperature range of 298 to 1273 K.

compact partially produced larger pores in the degreased compact and the final porous body.

A solid circle for each ball-milling time in Fig. 9 denotes a porosity of the fabricated porous body calculated from an ideal density of CCAS. The porosity was considered to be the sum of the volumes of open and closed pores, and it increased by increasing the ball-milling time. On the other hand, there was a difference between porosities investigated by the Hg intrusion method and ideal density, especially in case of ball-milling for 24 h. Since the Hg intrusion method clarifies volume for open pores in the porous body, the difference between values for open (○) and closed (●) pores was due to a ratio of closed pores in the porous body. Therefore, the difference in the case of ball-milling for 24 h, means that the ratio of the volume of the closed pores in the porous body was larger than that in cases of the ball-milling for 36 and 48 h. The extent of the closed pores in the porous body was considered to correspond to the existence of the agglomerated particles of the calcined powder, and the open pores in the porous body was found to increase by increasing the ball-milling time for the calcined powder.

The porous bodies of CCAS fabricated via the 36 h-ball-milling with almost homogeneous pore-size distribution had a low thermal expansion coefficient of $1.405 \times 10^{-6}/\text{K}$ in the temperature range of 298 to 1273 K, as shown in Fig. 10. Additionally, there was no hysteresis in the thermal expansion. A pore size of $0.375 \mu\text{m}$ which the porous body had was effective for capturing PM1 in polluted air; however, it was thought that a further decrease in the number of Cs^+ ions in aluminosilicate by a Ca substitution would be necessary to apply this material to a porous ceramic filter.

4. Conclusions

In this work, the effect of ball-milling in a PMMA solution on the amorphous calcined powder for the structure of porous bodies with the chemical composition $\text{Cs}_{0.74}\text{Ca}_{0.08}\text{Al}_{0.9}\text{Si}_{2.1}\text{O}_6$ (CCAS) was investigated. The ball-milling time for the amorphous powder calcined at 1073 K increased from 24 to 48 h, the pore size decreased from 0.71 to $0.159 \mu\text{m}$ and porosity increased from 47.4 to 52.9%. Additionally, the larger pore size greater than $1 \mu\text{m}$ disappeared as a result of the ball-milling, and resulted in an almost homogenous porous

structure. Amorphous calcined CCAS powder had a network of (Si, Al)O₄ tetrahedra similar to an aluminosilicate framework of leucite compounds and enhanced sinterability in comparison with the 9CAS. The porous bodies of CCAS fabricated via a 36 h-ball-milling treatment, with an almost homogeneous pore-size distribution, had a low thermal expansion coefficient of $1.405 \times 10^{-6}/\text{K}$ in temperatures ranging from 298 to 1273 K.

Acknowledgements This work was partially supported by the Mukai Science and Technology Foundation and by Grant-in-Aid No. 17750192 for Science Research from the Ministry of Education, Culture, Sports, Science, and Technology of Japan.

References

- 1) Hildemann, L. M., Markowski, G. R., Jones, M. C. and Cass, G. R., *Aerosol Sci. Tech.*, Vol. 14, pp. 138–152 (1991).
- 2) Lin, J. J. and Lee, L.-C., *Atmospheric Environment*, Vol. 38, pp. 469–475 (2004).
- 3) Ruiz, J. C., Blanc, Ph., Prouzet, E., Coryn, P., Laffont, P. and Larbot, A., *Separation and Purification Tech.*, Vol. 19, pp. 221–227 (2000).
- 4) Yanase, I., Tamai, S., Matsuura, S. and Kobayashi, H., *J. Eur. Ceram. Soc.*, Vol. 25, pp. 3173–3179 (2005).
- 5) Matsunuma, K., Ihara, T., Ban, S., Nakajima, S. and Okamoto, S., *JSAE Rev.*, Vol. 16, pp. 312–312 (1999).
- 6) Kobayashi, H., Terasaki, T., Mori, T., Yamamura, H. and Mitamura, T., *J. Ceram. Soc. Japan*, Vol. 99, pp. 686–691 (1991).
- 7) Yanase, I., Ishikawa, Y., Matsuura, S. and Kobayashi, H., *J. Eur. Ceram. Soc.*, Vol. 26, pp. 475–479 (2006).
- 8) Yanase, I., Tamai, S. and Kobayashi, H., *J. Ceram. Soc. Japan*, Vol. 111, pp. 533–536 (2003).
- 9) Dervine, R. A. B., *J. Non-Cryst. Solids*, Vol. 152, pp. 50–58 (1993).
- 10) Rokita, M., Handke, M. and Mozgawa, W., *J. Mol. Struct.*, Vol. 511/512, pp. 277–280 (1999).
- 11) Handke, M. and Mozgawa, W., *Vib. Spectr.*, Vol. 5, pp. 75–84 (1993).
- 12) Mozgawa, W., *J. Mol. Struct.*, Vol. 596, pp. 129–137 (2001).